International Journal of Hydrogen Energy 164 (2025) 150832

Contents lists available at ScienceDirect

International Journal of Hydrogen Energy

journal homepage: www.elsevier.com/locate/he

Dynamic assessment of decentralized hydrogen production and storage on a semi-submersible floating wind turbine platform

Thanh Dam Pham [a,b], Van Nguyen Dinh [c,d], Luan Cong Trinh [e], Frances Judge [a,b], Paul Leahy [a,b,*]

[a] MaREI Centre, Sustainability Institute, University College Cork, Cork, Ireland
[b] School of Engineering and Architecture, College Road, University College Cork, Cork, Ireland
[c] OWC, ABL Group, Ireland
[d] OWC, ABL Group, Viet Nam
[e] Technological University of the Shannon: Midlands Midwest, Limerick, Ireland

A R T I C L E I N F O

Handling Editor: Ramazan Solmaz

Keywords:
Decentralized offshore energy system
OpenFAST simulation
Green hydrogen production offshore
Fully-coupled analysis
VolturnUS-S semi-submersible platform
Floating offshore wind turbine

A B S T R A C T

Many offshore areas with significant wind resources are located far from electricity demand centers and existing energy transmission networks. Production of hydrogen directly on floating wind turbines is a scalable and modular approach to harnessing these wind resources. This paper presents a design for a floating 15 MW semi-submersible offshore turbine integrated with electrolyzers for hydrogen production and storage tanks. The modified configuration's hydrodynamic performance is simulated under combined aerodynamic and hydrodynamic loading conditions. The modifications led to a 4–5 % increase in pitch and roll inertia of the platform. The maximum acceleration at the nacelle increased by less than 10 %, remaining within acceptable limits, and the maximum power output changed by less than 2 % across all load cases. Mooring line tensions increased by approximately 3 %, demonstrating minimal impact on overall stability. The study demonstrates that onboard hydrogen integration can be achieved without compromising the dynamic response or energy production performance of the floating platform, supporting its viability as a decentralized offshore hydrogen production solution.

1. Introduction

The global energy landscape is increasingly shifting toward renewable sources in response to mounting concerns about climate change and the growing need for sustainable energy production [1,2]. Offshore wind power has gained recognition as a highly promising solution, capitalizing on the vast wind resources available over the ocean [3]. The worldwide offshore wind resource in areas of water depths of 50m–200 m within 92.6 km of the shore has been estimated 87 PWh per annum [4]. However, the deployment of wind turbines in deeper waters introduces substantial challenges [5–7]. To overcome these obstacles, floating offshore wind turbines (FOWTs) have been developed, offering greater flexibility in site selection and improved access to wind resources [8,9].

Green hydrogen is produced from time-varying renewable electricity through electrolysis, transforming it into stable chemical energy [10]. The hydrogen produced can be stored and later used to generate power in fuel cells or other systems, creating a closed loop between renewable eletricity and hydrogen, potentially addressing periodic deficits in electricity production from variable renewable sources. Hydrogen generated through electrolysis can also be used across various demand sectors, including power generation, construction, transportation, and industry.

In addition to the ongoing efforts to reduce the levelized cost of energy (LCOE) from floating offshore wind energy, a particularly promising approach to increasing the overall capture of offshore wind resources lies in the integration of FOWTs with hydrogen production and storage systems. Such integrated solutions offer an approach to overcoming the challenges of renewable energy utilization and storage [11]. Rodríguez Castillo et al. [12] provide a comprehensive review of offshore structural challenges and highlight the potential of combining hydrogen technologies with offshore renewable systems to overcome intermittency and improve system-level resilience. Their work emphasizes the need for robust design and operational strategies for platforms

* Corresponding author. MaREI Centre, Sustainability Institute, University College Cork, Cork, Ireland.
E-mail address: Paul.Leahy@ucc.ie (P. Leahy).

https://doi.org/10.1016/j.ijhydene.2025.150832
Received 28 March 2025; Received in revised form 21 July 2025; Accepted 2 August 2025
Available online 7 August 2025

supporting hydrogen production, compression, and storage in harsh marine environments. Zhang et al. [13] further stress the advantages of integrating superconducting wind generators with hydrogen production systems to maximize conversion efficiency and reduce transmission losses, supporting fully offshore energy independence. By coupling wind energy generation directly with hydrogen technologies, this approach addresses the variability of renewable energy sources while providing a stable and high-density alternative energy vector.

Ibrahim et al. [14] explores three concepts for integrating floating offshore wind (FOW) involving hydrogen generation strategies such as centralized onshore electrolysis, centralized offshore electrolysis, and decentralized offshore electrolysis systems. In the centralized onshore electrolysis configuration, electrical power generated by the floating offshore wind (FOW) farm is transmitted to land via subsea cables and utilized at an onshore facility for hydrogen production. This arrangement enables the deployment of high-capacity and high-efficiency electrolyzer systems, free from spatial and structural limitations associated with offshore installations. Alternatively, the centralized offshore electrolysis concept integrates the electrolysis process on a dedicated offshore platform, with hydrogen subsequently transported to shore through subsea pipelines or compressed hydrogen storage tanks [15]. While this approach simplifies maintenance by consolidating operational components, it also introduces a critical vulnerability due to its dependence on a single centralized unit. The decentralized offshore electrolysis concept involves hydrogen production directly on floating turbine platforms, with hydrogen piped to shore. This modular approach provides redundancy and potential cost savings by reducing the need for extensive electrical infrastructure.

Building on the integration of floating offshore wind turbines with hydrogen production, a decentralized hydrogen production architecture provides a promising pathway to address the intermittent nature of wind energy generation. For the widespread adoption of this integrated system, advanced hydrogen storage solutions are essential. Two primary methods are considered for transmitting hydrogen produced by a decentralized hydrogen production system. The first method is direct injection into pipelines for transport to shore, as introduced by the Dolphyn project [16,17]. The second method compresses hydrogen and stores it in tanks located on the floating platforms, followed by transportation to shore via hydrogen transport vessels. This option unlocks locations with strong wind resources but where construction of pipelines to shore would be impractical or too expensive. An optimal storage capacity of approximately seven days is recommended to manage supply effectively [18].

There are four primary floating platform concepts for FOWTs including spars, barges, semi-submersibles, and tension leg platforms (TLP). Barges [19,20] and semi-submersible platforms such as WindFloat [21], the OO-star model [22], the UMaine VolturnUS-S semi-submersible model [23], and the GustoMSC Tri-Floater [24] offer stability through their large mass and large water surface area. Spars [25,26] achieve stability through a slender cylindrical structure, which the center of gravity is positioned below the center of buoyancy. This configuration is typically enhanced using heavy ballast, such as concrete, placed at the bottom of the structure to lower the center of mass and improve righting stability. TLPs [27,28] rely on tensioned mooring systems for stability, making their design more complex due to the need for precise mooring. Spars are limited in deck space, making them unsuitable for accommodating additional equipment, and are particularly sensitive to added mass due to their small water plane area. TLPs are sensitive to changes in overall system mass, as such changes can alter the tension in the mooring system, potentially compromising stability. The installation of hydrogen production system equipment and storage tanks on platforms requires ample space for both installation and maintenance, with minimal sensitivity to mass increases, whether from hydrogen storage or adjustments in ballast mass to maintain the design draft of an FOWT system. Therefore, barges and semi-submersible platforms are more suitable for the decentralized hydrogen production concept, as they provide the necessary stability and space.

The electrolyzer is the key component in green hydrogen production, with four main types: Polymer Electrolyte Membrane (PEM), Alkaline Electrolyzed Cell (AEC), Anion Exchange Membrane (AEM), and Solid Oxide Electrolysis Cell (SOEC). The PEM electrolyzer provides benefits such as a small footprint and high output pressure and rapid response to load changes [29,30]. AEC, a well-established technology, offers high hydrogen production capacity, low investment costs, and a long operational lifespan. AEM and SOEC are still in the development phase with lower technology readiness levels (TRLs).

Hydrogen storage is a critical component in the development of a sustainable hydrogen economy, especially for offshore applications where space and weight constraints are significant. Various storage methods have been explored, each with its advantages and challenges [31]. Compressed hydrogen storage is widely used due to its simplicity and high gravimetric density [32]. Liquid hydrogen offers higher energy density but necessitates cryogenic temperatures, leading to increased energy consumption for liquefaction and insulation challenges [33]. Metal hydrides provide safe and compact storage options [31,34], but their heavy weight and slow uptake/release kinetics make them less suitable for dynamic offshore environments. Liquid organic hydrogen carriers (LOHCs) present a promising alternative, allowing hydrogen to be stored and transported under ambient conditions, though the hydrogenation and dehydrogenation processes require efficient catalysts and thermal management [34]. For floating offshore platforms, compressed hydrogen storage is currently the most viable options, balancing energy density, safety, and operational practicality.

This paper introduces a decentralized concept for integrating hydrogen production and storage on a 15 MW semi-submersible FOWT platform. The system employs PEM electrolysis for on-site hydrogen generation and lightweight composite tanks for high-pressure storage, eliminating the need for subsea cabling and enabling deployment in remote offshore locations. The integrated configuration is evaluated through coupled wind, wave, and hydrodynamic simulations to assess its impact on platform dynamics, stability, and operational performance. The key contributions include demonstrating the technical feasibility of hydrogen integration with floating wind, quantifying its effects on system response, and evaluating the performance of onboard storage under varying load scenarios. The paper is structured as follows: Section 2 describes the hydrogen-integrated platform and mooring system; Section 3 outlines the numerical methodology and design load cases; Section 4 presents dynamic analysis results; Section 5 discusses the impact of hydrogen system integration; Section 6 investigates the sensitivity to hydrogen storage conditions (full vs. empty); and Section 7 concludes with key findings and future research directions.

2. System description

This section provides a comprehensive description of the decentralized offshore hydrogen production and storage system proposed in this study. Key technical parameters and component specifications essential to the current analysis are detailed. The overall configuration and operational concept of the system are illustrated in Fig. 1. Electricity generated from the floating offshore wind turbine is utilized by onboard electrolyzers to produce hydrogen directly at the turbine location. Subsequently, the generated hydrogen is compressed and stored onboard in high-pressure composite tanks. To facilitate the hydrogen transportation process, specialized marine service vessels periodically collect stored hydrogen from individual floating platforms, delivering it to onshore receiving terminals for further distribution and utilization.

2.1. Floating offshore wind turbine

The wind turbine considered in this study is the IEA-15-240-RWT, a 15 MW reference wind turbine developed by the International Energy Agency (IEA) [35] to support research on modern floating offshore wind

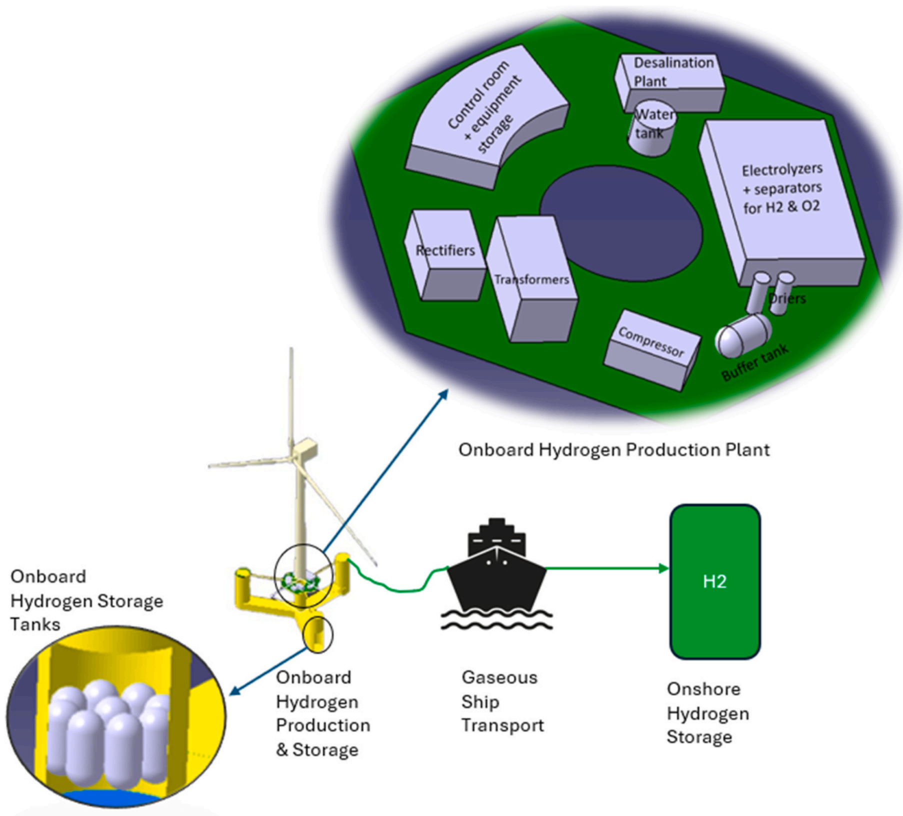

Fig. 1. Schematic of the decentralized offshore hydrogen production and storage concept.

systems. This open-source model features a three-bladed, upwind rotor configuration and employs variable-speed and collective pitch control strategies to optimize power generation and efficiency. The detailed specifications are provided in Table 1.

A semi-submersible floating platform was selected for integrating the wind turbine and hydrogen production and storage systems. The platform is based on the UMaine VolturnUS-S Reference Platform [23]. As shown in Fig. 2, the VolturnUS-S platform is engineered to achieve optimal stability and durability in harsh offshore environments.

Table 2 presents a comparison between the original platform and the modified floating platform (FWHS), which consists of an FOWT integrated with hydrogen production and storage systems. To maintain a constant total platform mass, the additional weight from the extended deck, hydrogen storage tanks, hydrogen production plant, and associated subsystems is compensated by reducing the fluid ballast weight accordingly. The center of gravity (COG) of the FWHS is higher than the original model and the mass of steel in the platform increases by 8 % due to the extended deck and its support structure.

Table 1
Specifications of the 15-MW reference offshore wind turbine [35].

Wind turbine properties	Unit	Value
Rated power	MW	15
Rotor	–	3 blades, up wind
Wind turbine control	–	Collective pitch, Variable speed
Rotor diameter	m	240
Hub height	m	150
Cut-in/rated/cut-out wind speed	m/s	3/10.6/25
Rotor speed at rated power	rpm	7.56
Rotor nacelle assembly mass	ton	991
Tower mass	ton	1263

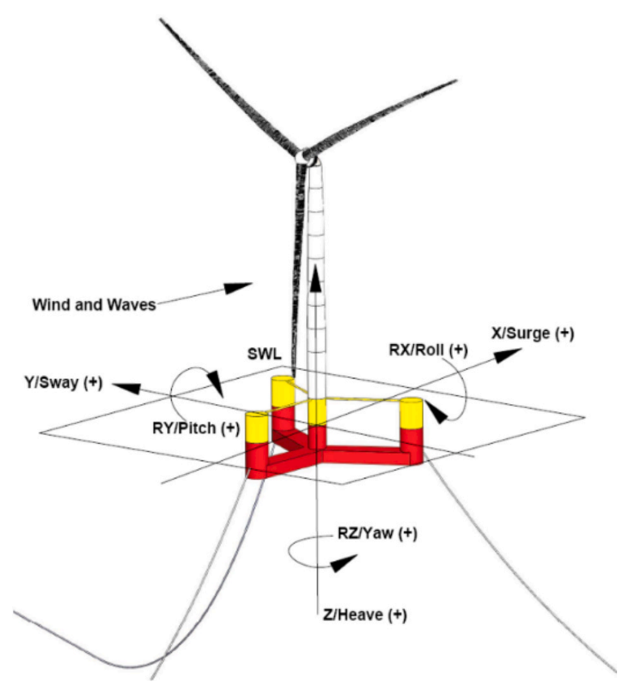

Fig. 2. The UMaine VolturnUS-S reference platform supporting the IEA-15-240 reference wind turbine system [23].

2.2. Hydrogen production and storage systems

Fig. 3 shows a schematic diagram of the hydrogen production and storage system on the floating offshore wind turbine, while details the subsystems of the electrolyzer plant on the extended deck. The storage

Table 2
Modified FWHS semi-submersible floating platform specifications and difference from the unmodified VolturnUS-S

Platform properties	Unit	VolturnUS-S	FWHS	Difference
Vertical COG from still water level	m	−14.94	−14.01	−6 %
Hull volume displacement	m^3	20,206	20,206	0 %
Platform mass	ton	17,754	17,754	0 %
Inertia about COG - Ixx	kgm^2	1.25×10^{10}	1.31×10^{10}	4 %
Inertia about COG - Iyy	kgm^2	1.25×10^{10}	1.31×10^{10}	5 %
Inertia about COG - Izz	kgm^2	2.37×10^{10}	2.37×10^{10}	0 %
Platform steel mass	ton	3914	4240	8 %
Fix ballast mass	ton	2540	2540	0 %
Fluid ballast mass	ton	10,509	9990	−5 %

tanks are installed within the side columns of the floating platform as shown in Fig. 4.

The wind turbine harnesses wind energy to generate electricity, which undergoes voltage adjustment through a transformer. This transformer is required to deliver the correct voltage for the electrolysis process. Following this, a rectifier is employed to convert the AC (alternating current) electricity into a stable, consistent DC (direct current) output, a necessary step since the electrolyzer is a DC device.

The desalination plant plays a vital role in the electrolysis process by converting seawater into fresh water, a necessary requirement in offshore environments. The fresh water produced is stored in a water tank, which is responsible for providing a constant and stable supply of water to the electrolyzer. The tank capacity is specified in order to ensure an adequate water supply for the hydrogen system to operate at full capacity for up to 4 h.

The electrolyzer, powered by rectified DC electricity, separates water into hydrogen and oxygen. In this concept only the hydrogen is collected for use, while the oxygen byproduct is safely released into the atmosphere. This study is based on a PEM electrolyzer Silyzer 300 (Siemens, Germany) [36], which is particularly suited for offshore environmental conditions due to its compact design and ability to operate under variable power inputs. The choice of PEM technology in this study reflects recent advances in its technical maturity and suitability for the demanding conditions of offshore hydrogen production from a time-varying power source [37].

The hydrogen gas produced by the electrolyzer usually contains moisture that must be removed for further processing. Drying units are employed to eliminate this moisture, thus purifying the hydrogen to a level suitable for storage. The purified hydrogen is then held in a buffer tank which regulates the flow of hydrogen into the compressor. The hydrogen is then compressed to approximately 70 MPa. Hydrogen compression technologies are broadly classified into mechanical and non-mechanical types. Mechanical compressors include reciprocating, diaphragm, linear, and liquid compressors, while non-mechanical compressors include cryogenic, metal hydride, electrochemical, and adsorption compressors [38]. In this study, we reference the MAX Compression System 2.0 (Maximator, Germany), which is a two-stage reciprocating compressor driven by hydraulics [39].

Hydrogen storage tanks are categorized into five types based on their material composition [40]. Type I tanks are entirely metal, typically steel or aluminum, and are primarily used in stationary applications due to their high mass. Type II tanks are similar but include a composite wrap around the metal liner, enabling higher pressure storage. Type III tanks feature a metallic liner encased in a composite material, striking a balance between strength and weight, making them ideal for vehicular applications. Type IV tanks, which use a polymeric liner with a

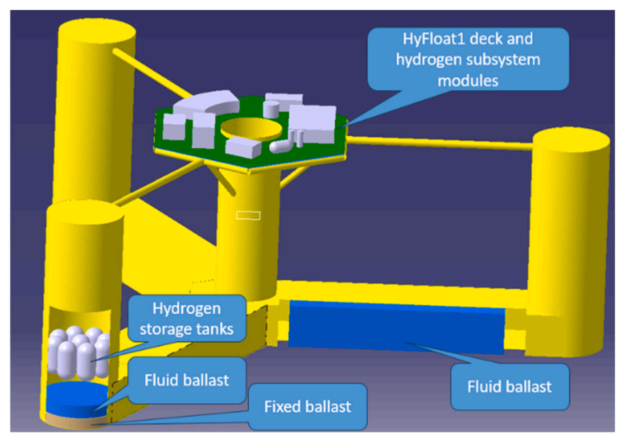

Fig. 4. View of modified VolturnUS-S platform showing the extended deck for hydrogen production and embedded storage.

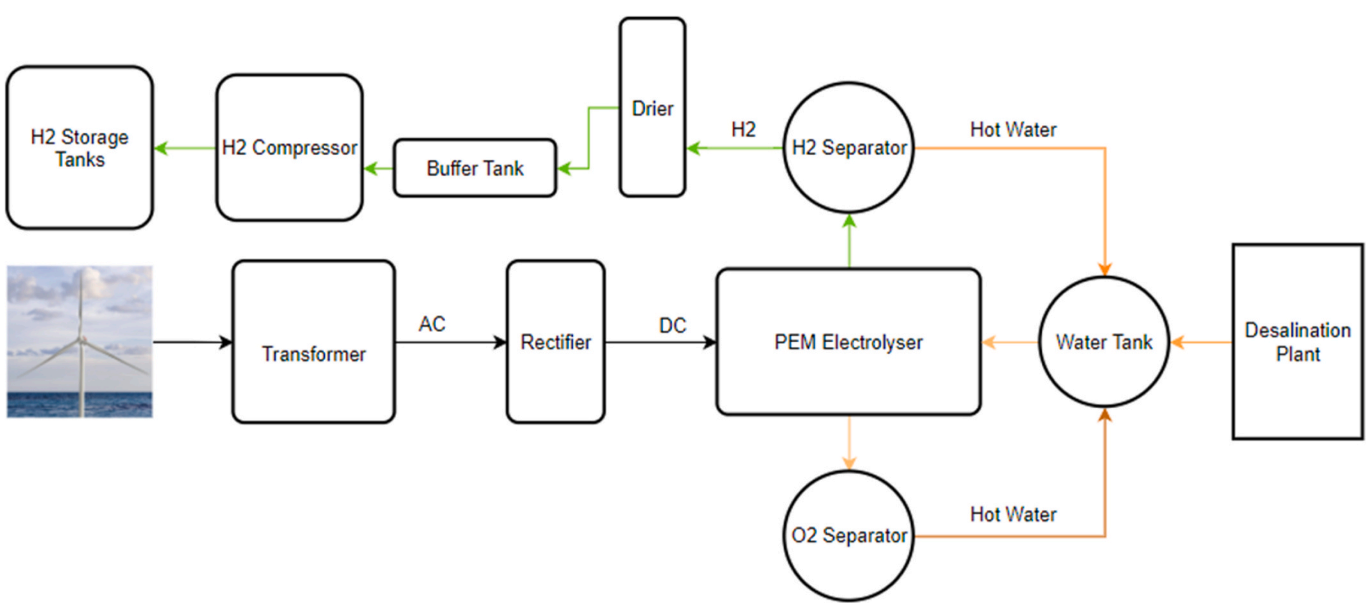

Fig. 3. Hydrogen production and storage system scheme on a floating offshore wind turbine platform.

composite wrap, further reduce weight while maintaining high-pressure storage capabilities. Type V tanks are fully composite, without any metallic or polymer liner, designed for high-pressure applications but still in development and not yet widely adopted due to their high costs. In this study, Type IV tanks were chosen to store hydrogen compressed at 70 MPa, with the tanks distributed across the three side columns of the platform.

Efficient offloading of stored hydrogen is vital for the continuous operation of the floating offshore hydrogen production system. This process uses a flexible pipe connection to transfer compressed hydrogen from the platform storage tanks to a transport vessel that periodically docks alongside the platform. The offloading system is not the focus of this study, however it should be noted that it would be specified to handle dynamic offshore conditions, ensuring a secure and steady flow of hydrogen while accommodating the movements of both the platform and vessel. This transmission method reduces the need for extensive offshore infrastructure and supports continuous energy production by aligning offloading frequency with storage capacity and production rates.

Storing hydrogen at 70 MPa onboard floating platforms introduces safety challenges, including risks of leakage, explosion, and structural damage from dynamic marine conditions. To mitigate these risks, systems should incorporate pressure relief valves, gas detectors, and follow offshore standards like ISO 11119 and ISO 11439 [40,41]. Key concerns include fatigue loading, corrosion, and safe offloading operations. While this study focuses on technical feasibility, future work should include detailed failure mode analysis and safety planning to ensure reliable offshore deployment.

Table 3 provides an overview of the primary components involved in a hydrogen production and storage system, detailing their quantities, specifications, total mass, and the vertical center of gravity (COG_z). The data illustrates the distribution of mass and vertical positioning of each component, and a summary specification of the main equipment required. In order to size the storage tanks, assumptions for some key operational metrics of a wind turbine-powered hydrogen production and storage system are proposed in Table 4. With a capacity factor (CF) of 0.6, the wind turbine would generate 216 MWh of electricity on a typical day, supporting the production of approximately 3200 kg of hydrogen daily. The system compressor would handle a mass flow rate of 276 kg of hydrogen per hour, facilitating the storage of hydrogen in high-pressure tanks with a total capacity of 28,700 kg at 70 MPa. At full production capacity, it would take about 9 days to completely fill the storage tank.

Table 3
Specification of hydrogen subsystem modules

Equipment	Quantity	Spec	Total Mass (ton)	COG_z (m)
Transformer	1 set	15 MVA	27	14.80
Rectifier	1 set	12 MVA	21	14.80
Electrolyzer	1	Siemens Sylizer 300 (4 arrays), Total power demand 11.7 MW, dry gas quality 99.9999 % Start-up time <1 min	70	15.95
Dryer	2	3.5 MPa input, 3.5 MPa output	8	16.15
Buffer tank	1	3.5 MPa	10	15.80
Compressor	3	MAX compression system 250 kW Mass flow 92 kg/h @3.5 MPa inlet working pressure 90 MPa	46	15.85
Water tank	1	15m^3	15	15.93
Fresh water generator	3	Wartsila freshwater generator model SSD2-4, 30–35 m^3/day	2	15.80
Frame, pipe & outfitting	1		100	15.85
Control room	1		10	15.80
Deck	1	700 m^2	330	14.10
Storage tanks	27	Carbon fiber and polyethylene liner, tank volume 27,254 m^3	675	−9.20
Subtotal system			1314	2.51

2.3. Station-keeping system

The floating platform is secured using a three-line catenary mooring system, designed to ensure stability under offshore environmental conditions. The mooring lines, composed of R3 studless chain, are evenly distributed at 120-degree intervals around the platform. Each mooring line has a nominal diameter of 185 mm and an unstretched length of 850 m, with fairleads positioned 14 m below the still water level. Additional specifications are detailed in Table S1.

3. Methodology

The floating wind turbine model used in this study is based on the publicly available VolturnUS-S semi-submersible platform coupled with the IEA 15 MW reference turbine, developed and verification by the National Renewable Energy Laboratory (NREL) [42]. This high-fidelity model serves as a standardized benchmark for floating offshore wind system research and has undergone extensive verification through numerical and experimental studies as documented in the NREL definition report [23]. In this work, the hydrogen-integrated FWHS system is constructed by modifying this baseline configuration to include onboard hydrogen production and storage systems. All simulations are performed using OpenFAST, and the impact of the integration is assessed by directly comparing the dynamic responses of the FWHS model with the original VolturnUS-S model. To ensure consistency and generality, the effects are quantified in a non-dimensional form, enabling a clear evaluation of changes in system behavior attributable solely to the hydrogen system integration.

A FOWT system is subjected to environmental forces from wind, waves, and ocean currents, which vary based on the deployment location. The primary loads acting on the system are governed by aerodynamic, hydrodynamic, and mooring restoring forces. The fully coupled dynamic response of the FOWT in the time domain is governed by the following Equation (1).

$$M_{ij}\ddot{x}_j(t) = \sum F_i(t) \quad (1)$$

where M_{ij} represents the mass and mass inertia matrix of the floating wind turbine, the total external force matrix $\sum F_i(t)$ is composed of multiple contributing forces including hydrodynamic forces F_i^H (t), aerodynamic loads F_i^W (t), viscous drag forces F_i^V (t) described by Morison's equation, and mooring system restoring forces F_i^M (t). The summation of these forces is given by Equation 2.

$$\sum F_i(t) = F_i^H(t) + F_i^W(t) + F_i^V(t) + F_i^M(t) \quad (2)$$

Table 4
Hydrogen production and storage calculation

Average wind turbine power generation per day (capacity factor CF = 0.6)	216	MWh/day
Average H_2 production per day	3200	kgH_2/day
Compressor mass flow	276	kgH_2/h
Hydrogen storage tank capacity @70 MPa	28,700	kg H_2
Time to fill hydrogen storage tank	9.0	day

3.1. Aerodynamic forces

The aerodynamic forces acting on the turbine rotor blades are evaluated using the blade element momentum (BEM) theory [41]. This method discretizes each blade into multiple segments, allowing for the calculation of aerodynamic forces on each element, which are then integrated to determine the total forces and moments acting on the rotor.

The incremental thrust (dT) and torque (dQ) generated by each blade element are computed using Equations (3) and (4).

$$dT = \frac{1}{2}\rho_a V_{rel}^2 (C_L \cos\phi + C_D \sin\phi) c\, dr \tag{3}$$

$$dQ = \frac{1}{2}\rho_a V_{rel}^2 (C_L \sin\phi - C_D \cos\phi) c\, dr \tag{4}$$

where C_L and C_D represent the lift and drag coefficients, respectively. The relative flow velocity acting on the blade section is denoted by V_{rel}, with ø representing the local flow angle. Additionally, c corresponds to the chord length of the blade section and ρ_a indicates the density of air.

The aerodynamic forces acting on an airfoil depend on the velocity components and angles at each blade segment. These forces contribute to the overall thrust and torque exerted on the rotor, which are critical in defining the aerodynamic performance of the turbine. To enhance accuracy, the aerodynamic calculations also incorporate hub losses, tip losses, and skewed wake effects.

3.2. Hydrodynamic loads

The hydrodynamic behavior of a floating platform is influenced by multiple forces, including hydrostatic restoring forces, added mass effects, radiation damping, wave excitation forces, and viscous drag. The interaction between these forces determines the platform response to ocean conditions such as waves, currents, and buoyancy forces.

The hydrostatic restoring force arises from buoyancy and acts to return the platform to its equilibrium position when displaced. Wave radiation effects contribute to both added mass and damping forces, which influence the platform dynamic response. The first-order wave excitation force, generated by incident waves, affects platform motion. the second-order wave excitation forces result from nonlinear wave interactions, which can introduce low-frequency motions, particularly in deep water environments.

The total hydrodynamic force exerted on a FOWT can be represented by Equation (5).

$$F_i^{Hydro} = F_i^{Hydrostatic} + F_i^{Radiation} + F_i^{Wave(1)} + F_i^{Wave(2)} + F_i^{Drag} \tag{5}$$

Where:

$F_i^{Hydrostatic}$ represents the hydrostatic forces. The hydrostatic forces can be expressed as in Equation (6).

$$F_i^{Hydrostatic} = \rho g V_0 \delta_{i3} - C_{ij}^{Hydrostatic} x_j(t) \tag{6}$$

The term $C_{ij}^{Hydrostatic}$ contains the linear hydrostatic restoring coefficients as shown in Equation (7) with A_w as the water plan area, and Z_B and Z_G are vertical positions of center of buoyancy and gravity. The term $\rho g V_0 \delta_{i3}$ is valid in the vertical direction only. It represents the buoyancy force acting on a floating structure and is based on the density of water ρ, gravitational acceleration g, and displaced volume of the floating platform V_0 when it is undisplaced.

$$C_{ij}^{Hydrostatic} = \begin{bmatrix} 0 & 0 & 0 & 0 & 0 & 0 \\ 0 & 0 & 0 & 0 & 0 & 0 \\ 0 & 0 & \rho g A_w & \rho g \iint_{Aw} y dA_w & -\rho g \iint_{Aw} x dA_w & 0 \\ 0 & 0 & \rho g \iint_{Aw} y dA_w & \rho g \iint_{Aw} y^2 dA_w + \rho g V_0 (Z_B - Z_G) & 0 & 0 \\ 0 & 0 & -\rho g \iint_{Aw} x dA_w & 0 & \rho g \iint_{Aw} y^2 dA_w + \rho g V_0 (Z_B - Z_G) & 0 \\ 0 & 0 & 0 & 0 & 0 & 0 \end{bmatrix} \tag{7}$$

$F_i^{Radiation}$ accounts for radiation damping and added mass. The radiation forces, arising from wave interactions with the floating platform, include both added mass effects and wave radiation damping. These forces are proportional to the platform acceleration and velocity, and their contribution can be formulated by Equation (8).

$$F_i^{Radiation} = -A_\infty \ddot{x}_j(t) - \int_0^t \left[\frac{2}{\pi} \int_0^\infty B_{ij}(\omega) cos(\omega t) d\omega \right] \dot{x}_j(t-\tau) d\tau \tag{8}$$

where $A_{ij}(\infty)$ is the added mass at infinite frequency and the wave radiation damping is denoted by $B_{ij}(\omega)$.

The first-order wave excitation force $F_i^{Wave(1)}$ is caused by the incident wave field and can be expressed by Equation (9). The function $W(\omega)$ is the Fourier transform of a white Gaussian noise (WGN) time-series process characterized by a zero mean and unit variance, $S_\zeta^{2-side}(\omega)$ is the two-sided wave spectrum, $X_i(\omega,\beta)$ is a complex-value array representing the wave excitation force acting on the platform which depends on wave frequency ω and wave heading angle β.

$$F_i^{Wave(1)}(t) = \frac{1}{2\pi} \int_{-\infty}^{\infty} W(\omega) \sqrt{2\pi S_\zeta^{2-side}(\omega)} X_i(\omega,\beta) e^{j\omega t} d\omega \tag{9}$$

$F_i^{Wave(2)}$ corresponds to second order wave forces. Since the mooring system follows a catenary configuration, the platform exhibits significant low-frequency motions. As a result, slow-drift effects become more dominant in the system's dynamic response. Given this characteristic, only difference-frequency Quadratic Transfer Functions (QTFs) are considered, as they primarily influence the low-frequency motion components, while sum-frequency effects, which are typically associated with higher-frequency responses, are less relevant in this context. Therefore, $F_i^{Wave(2)}$ can be presented as in Equation (10) with the force coefficient X_{mk} corresponding to amplitude of incident waves A_m and A_k at frequencies ω_m and ω_k.

$$F_i^{Wave(2)} = Re\left(\sum_{m=1}^{N} \sum_{k=1}^{N} A_m A_k^* X_{mk} e^{j(\omega_m - \omega_k)t} \right) \tag{10}$$

F_i^{Drag} denotes nonlinear viscous drag forces. The viscous drag forces are described by Morison's equation, which is dependent on the square of the relative velocity between the water particles and the floating structure as shown in Equation (11), where C_D is the drag coefficient, A

is the projected area of the structure in the flow direction, $v_i(t)$ is the velocity of water particle.

$$F_i^{Drag} = -\frac{1}{2}C_D\rho A\left(u_i(t) - \dot{x}(t)\right)\left|v_i(t) - \dot{x}(t)\right| \quad (11)$$

3.3. Mooring dynamic loads

The mooring system exerts both static and restoring forces, which are typically represented using a linear model, making it suitable for frequency domain analysis. Mooring line tension can be determined using either a quasi-static method or a dynamic approach. To accurately capture the mooring system's effects in the time domain, the dynamic mooring line force must be incorporated into the analysis. Hall proposed a lumped mass model to simulate the dynamic behavior of mooring lines attached to floating offshore structures [42]. The nonlinear dynamic equation governing the motion of a mooring line segment is given by Equation (12).

$$M_m\ddot{x}(t) + C_m x(t) - F_B - F_G - F_D = f \quad (12)$$

Where M_m is the mooring mass matrix, which remains constant over time, and C_m is the mooring stiffness matrix, which varies based on the mooring line displacement. The terms F_B, F_G, and F_D are the buoyancy force, gravity force, and drag force, respectively.

3.4. Numerical simulation tool

In this study, the FWHS is analyzed using a fully integrated simulation frame work within OpenFAST. Developed by the National Renewable Energy Laboratory (NREL) since 2005 under Jonkman and Buhl Jr. [43], OpenFAST is an open-source tool designed for the comprehensive modeling of floating and fixed-bottom wind turbine systems. It enables fully coupled time-domain simulations, incorporating aerodynamics, structural elasticity, control systems, hydrodynamics, and mooring dynamics, as illustrated in Fig. 5.

The AeroDyn module calculates aerodynamic forces on wind turbines, using local blade motions and velocities at each time step to compute forces and moments, also calculates generator torque, rotor thrust, and power coefficient. This module is integrated with TurbSim [44] to create turbulent wind fields for dynamic simulations.

The ServoDyn module manages control systems and actuators, simulating the dynamic response of control mechanisms such as blade pitch and generator torque controllers. This module ensures the interaction between the control systems and the mechanical components of wind turbine is accurately modeled.

The ElastoDyn module handles the structural elasticity of the wind turbine, modeling the dynamic response of the flexible components, including the blades, tower, and drivetrain. It uses inputs from other modules to simulate the structural behavior under various loads and conditions.

The HydroDyn module computes hydrodynamic loads considering first and second order wave forces, and viscous drag forces. Using platform-specific data such as member size and drag coefficients, HydroDyn evaluates hydrodynamic and hydrostatic forces, and the results are sent to OpenFAST for motion equation solving.

The MoorDyn module calculates dynamic mooring forces, requiring input parameters related to mooring line configuration and stiffness. It processes platform position and velocity data, solves the dynamic behavior of mooring lines, and provides the resulting mooring forces to OpenFAST, ensuring a fully coupled analysis of floating wind turbine systems.

3.5. Design load cases

To evaluate the impact of hydrogen production and storage systems on platform dynamics, six representative design load cases (DLCs) based on the VolturnUS-S platform [23] are simulated in OpenFAST. Results for the FWHS system are compared with the original model. Table 5 lists the DLCs, including operational conditions (DLC1.1, 1.3, 1.4, 1.6) and extreme environmental conditions with parked wind turbine cases (DLC6.1, 6.3) DLC1.1 uses the Normal Turbulence Model (NTM) to assess stability and power output under typical sea states. DLC1.3 uses the same sea conditions but replaces NTM with the Extreme Turbulence Model (ETM) to evaluate responses to wind variability. DLC1.4 simulates an Extreme Coherent Gust with Direction Change (ECD) to study dynamic loads from abrupt wind shifts. DLC1.6 also uses NTM but under harsher sea states to test performance under elevated loads.

DLC6.1 applies 50-year wind and wave conditions with an 8° yaw misalignment to assess structural response in extreme scenarios. DLC6.3 uses a milder 1-year sea state with 20° yaw to test structural integrity under high wind loading.

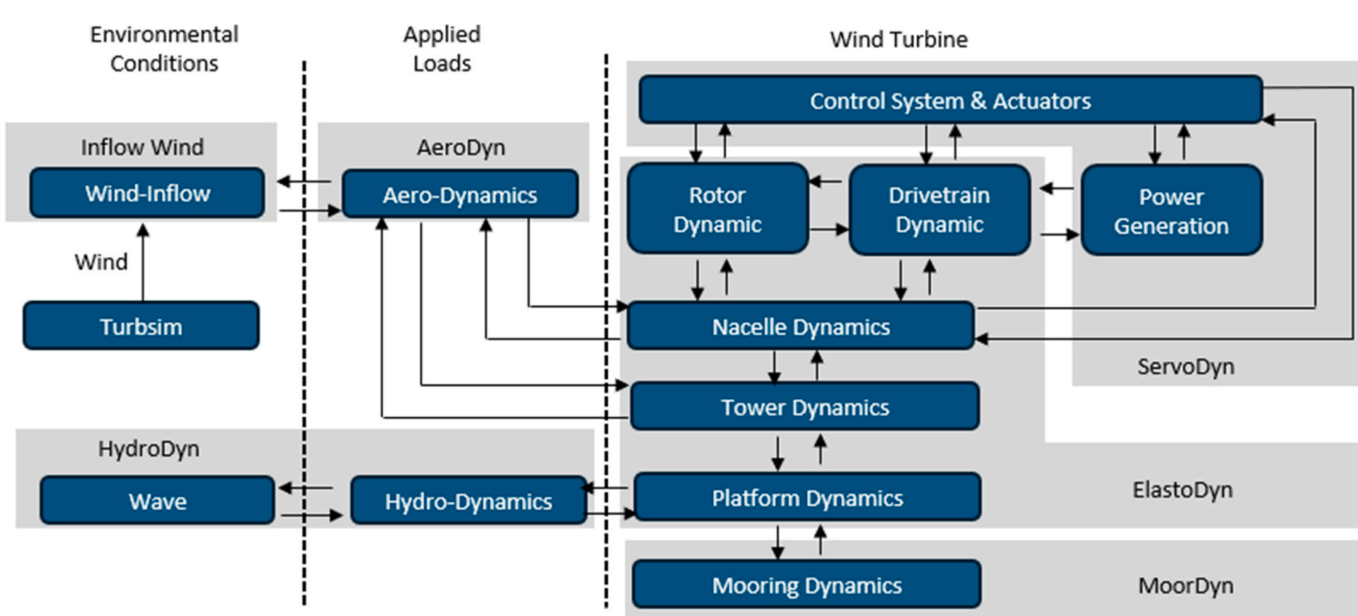

Fig. 5. Numerical simulation structure of OpenFAST.

Table 5
Design load cases [23].

Design load cases	Wind model	Wind speed at hub (m/s)	Wave Hs (m)	Wave Tp (s)	Setting	Wind turbine status
1.1/1.3	NTM/ETM	4	1.1	8.52		Operational
		6	1.18	8.31		
		8	1.32	801		
		10	1.54	7.65		
		12	1.84	7.44		
		14	2.1	7.46		
		16	2.6	764		
		18	3.06	8.05		
		20	362	8.52		
		22	4.03	8.99		
		24	4.52	945		
1.4	ECD ± R-2.0	8	1,32	801	+/− Dir. Change	
	ECD ± R	10	1.54	7.65	+/− Dir. Change	
	ECD ± R+2.0	12	1.84	7.44	+/− Dir. Change	
1.6	NTM	4	6.3	11.5		
		6	8	12.7		
		8	8	12.7		
		10	8.1	12.8		
		12	8.5	13.1		
		14	8.5	13.1		
		16	9.8	14.1		
		18	9.8	14.1		
		20	9.8	14.1		
		22	9.8	14.1		
		24	9.8	14.1		
6.1	EWM 50 yr	47.5	10.7	14.2	Yaw±8°	Parked, blade 90°
6.3	EWM 1 yr	38	6.98	11.7	Yaw±20°	

Hs: Significant wave height; Tp: Peak period of wave.
NTM/ETM: normal/extreme turbulence model.
EWM50: extreme wind speed model in 50 years return period.
ECD: Extreme Coherent gust with Direction change.

3.6. Modelling assumptions

To simplify the numerical modeling of the FWHS system while maintaining consistency with the verified baseline platform, the following assumptions are applied:

The environmental conditions are adopted from the original VolturnUS-S design and are representative of offshore sites along the U.S. East Coast.
The original structural geometry of the semi-submersible platform is retained. To maintain the same draft and preserve the platform's hydrodynamic characteristics, only the ballast water mass is adjusted.
The mooring system layout and parameters are kept unchanged.
The structural flexibility of the hydrogen storage tanks is not modeled; they are assumed to be fixed rigid bodies.
The effect of hydrogen mass variation during storage tank loading and unloading is neglected, as the total hydrogen mass constitutes a negligible fraction of the overall platform mass.

4. Dynamic analysis of system responses, wind turbine performance, and load assessment under various environmental conditions

Fig. 6 presents the dominant motions (surge, heave, and pitch) of the modified platform at the global origin, located at the center of the platform and the still water level, under critical load cases. In DLC1.6_12mps, the wind turbine operates near rated speed, experiencing maximum thrust. In DLC1.6_24mps the wind turbine operates near cut-out wind speed. In DLC6.1_8_47.4mps, the wind turbine is parked, with an 8-degree yaw relative to the wind direction. Three DLCs incorporate extreme irregular waves. Notably, surge and pitch motions are most significant under maximum wind turbine thrust (DLC1.6_12mps), reaching 22.5 m and 5.8°, respectively.

When evaluating the stability of hydrogen production systems and storage tanks, it is crucial to assess the acceleration at the specific locations of these devices on the platform. Figs. 7 and 8 present the acceleration data for the nacelle, hydrogen electrolyzer, and hydrogen storage tanks located at the downwind side column. These Figures display the acceleration parameters in both time series and power spectrum density formats. Fig. 7 illustrates acceleration under load case DLC1.6, characterized by an average wind speed of 24 m/s, a significant wave height (Hs) of 9.8 m and a peak period (Tp) of 14.1 s. Fig. 8 shows acceleration under load case DLC6.1, with an average wind speed of 47.5 m/s, a significant wave height of 10.7 m, and a peak period of 14.2 s.

Table S2 presents the maximum, minimum, and standard deviation of acceleration for the nacelle, hydrogen storage tanks, and electrolyzer in three directions (x, y, and z) under three DLCs. The nacelle experiences the highest accelerations in the x and y directions, particularly in x, due to its height (150 m above SWL) and sensitivity to pitch and roll motion. These accelerations increase under stronger winds and more extreme DLCs. The hydrogen storage tanks and electrolyzer have lower accelerations compared to the nacelle in the x and y-directions. The z-direction acceleration is similar for tanks and electrolyzer but higher than for the nacelle due to their off-center placement on the platform. The DLC 6.1 with 8° yaw angle results in the highest accelerations for all components, indicating that misaligned wind conditions induce higher accelerations than aligned ones. Examination of the standard deviation values reveals that the tank and electrolyzer accelerations are less sensitive to fluctuating wind and wave loads than the nacelle.

5. Impact of hydrogen production and storage systems on the FOWT

To evaluate the impact of the hydrogen production system and storage tanks on the FOWT system, simulations were conducted for both the FWHS and the original FOWT. An earlier study calculated the natural frequencies of six degrees of freedom of the platform [45], revealing that the integration of the hydrogen production system and storage tanks resulted in minimal changes to the platform's natural frequencies. To further assess the impact, the maximum values for each DLC were extracted from the time series outputs and compared. The ratios of these maximum values between the two models provide insights into the influence of the hydrogen production and storage system on the overall response of the FOWT.

Figs. 9 and 10 show the ratios of maximum values between FWHS and the original model across various DLCs. The integration of a FWHS system into the FOWT design introduces certain modifications to the platform's structural and dynamic behavior compared to the original model. Notably, the FWHS model experiences elevated loads,

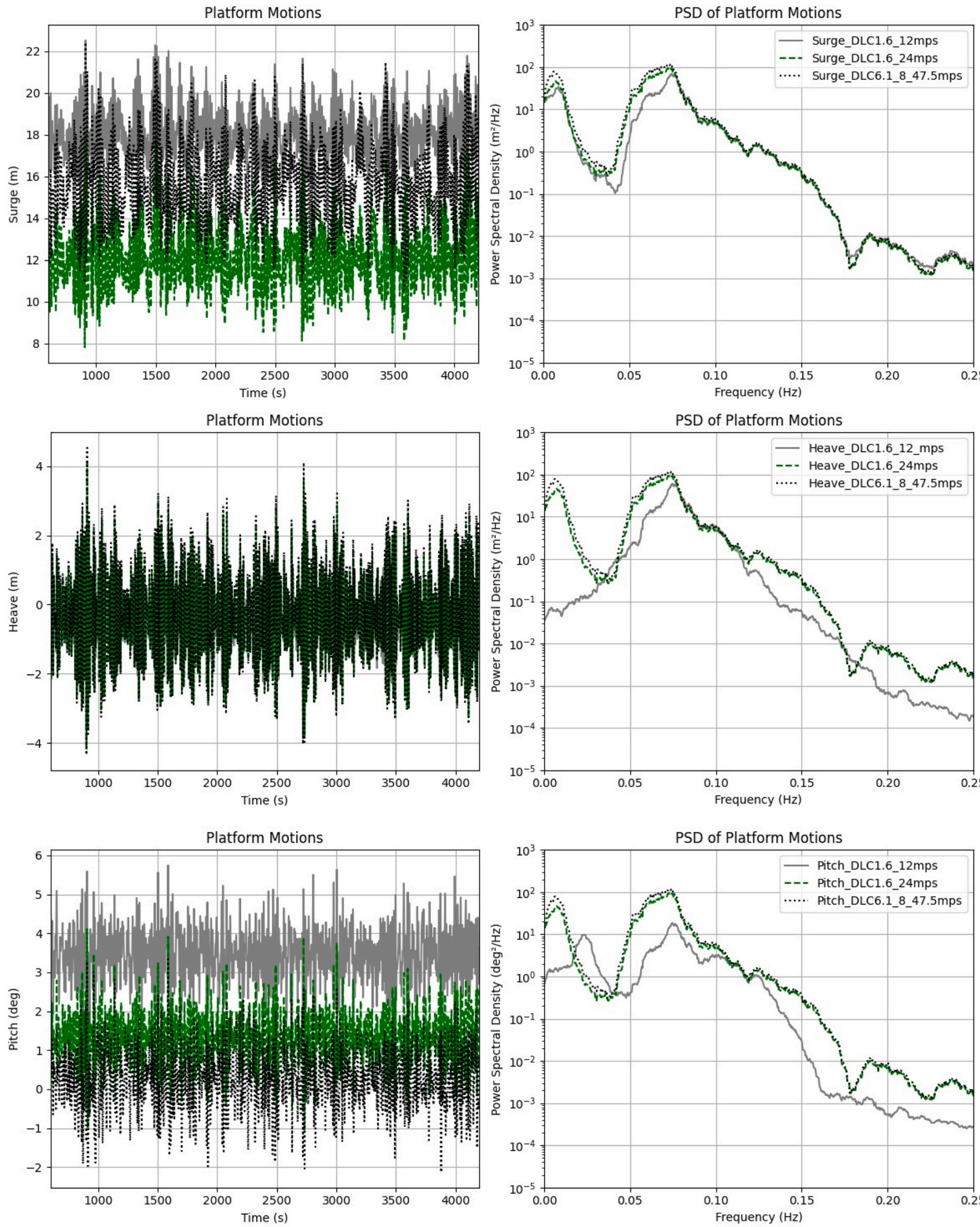

Fig. 6. Responses of the modified platform under critical load scenarios: surge, heave, and pitch in the time domain (left column) and frequency domain (right column).

particularly in terms of the tower base bending moment. This load increase is most pronounced under extreme wind and wave scenarios. The primary factor contributing to these heightened loads is the elevated COG in the FWHS model due to the added mass of the hydrogen production components at the extended deck and hydrogen storage tanks while reducing ballast mass at the bottom of the platform. The higher COG reduces the overall restoring moment of the system, making it more susceptible to pitch motions. Consequently, the platform experiences larger pitch angles, leading to increased accelerations and bending moments at the tower base.

The FWHS model exhibits slight changes in nacelle accelerations. Nacelle x-direction (Ax) acceleration increases by approximately 2 % in DLC1.1, DLC1.3, and DLC1.6, while the change is smaller in other DLCs. Nacelle y-direction (Ay) acceleration increases notably in DLC1.4, DLC1.6, and DLC6.1, reaching approximately 10 % in DLC1.4 due to wind direction changes or extreme wind conditions.

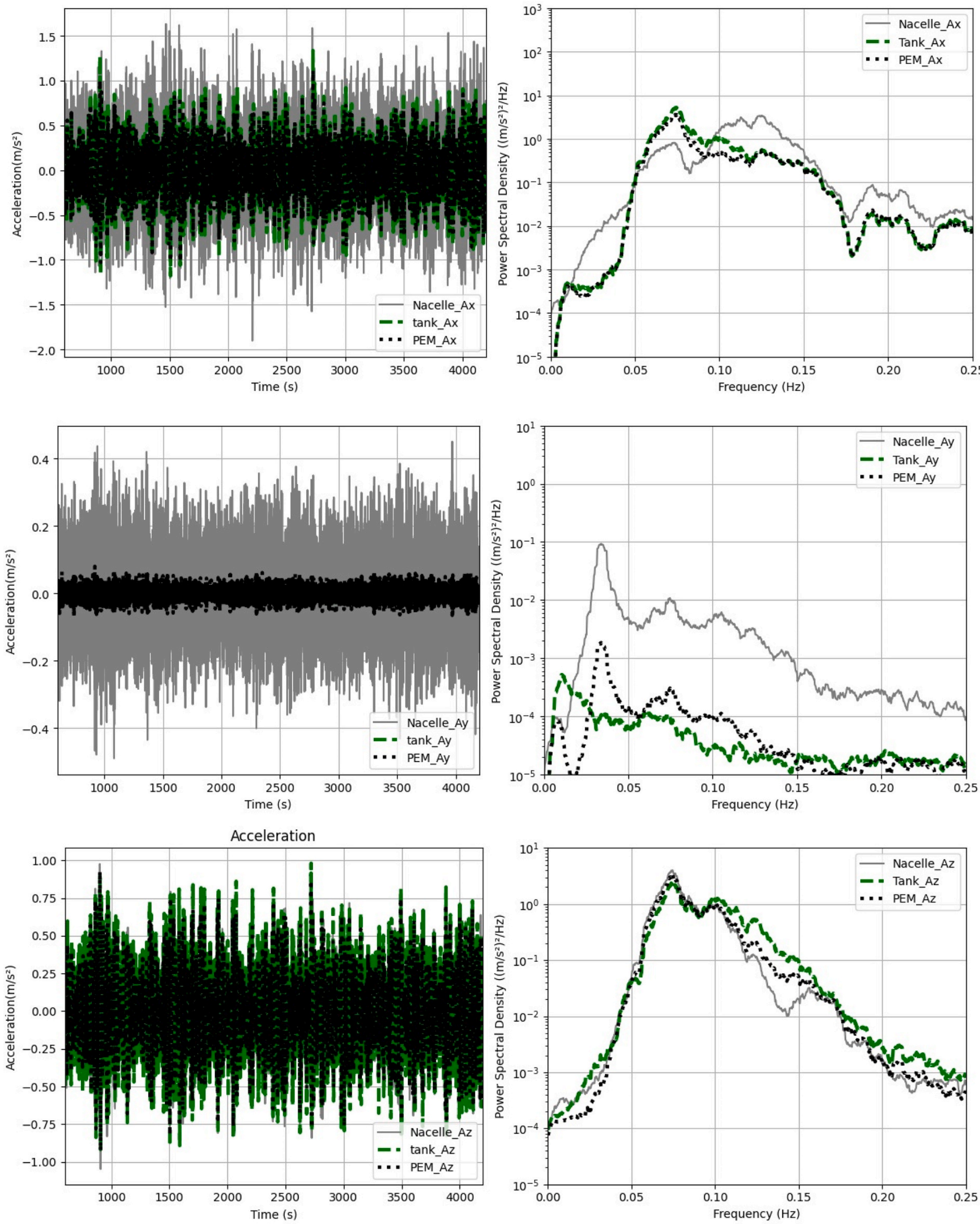

Fig. 7. Acceleration in x, y, and z directions of the nacelle, hydrogen tanks, and PEM module at 24 m/s wind speeds with irregular waves (Hs = 9.8 m, Tp = 14.1 s) in DLC1.6 conditions; time domain on the left column and frequency domain on the right column.

The power generation performance of the FWHS model remains largely unaffected, with less than a 2 % difference compared to the original design across all DLCs. This result is crucial in demonstrating that the integration of hydrogen production and storage does not compromise wind energy harvesting efficiency. Despite the increased loads, this observation confirms the viability and effectiveness of the FWHS concept. It also highlights the importance of addressing the structural challenges introduced by the additional system components while ensuring that the target power output is maintained.

Beyond the increased pitch motion and associated loads, the FWHS model exhibits similar dynamic behavior to the original model in terms of other motions, such as surge, heave. This similarity suggests the FWHS system does not substantially alter the overall dynamic response of the platform.

The mooring system of the FWHS model experiences slightly higher fairlead and anchor line tensions compared to the original model. The

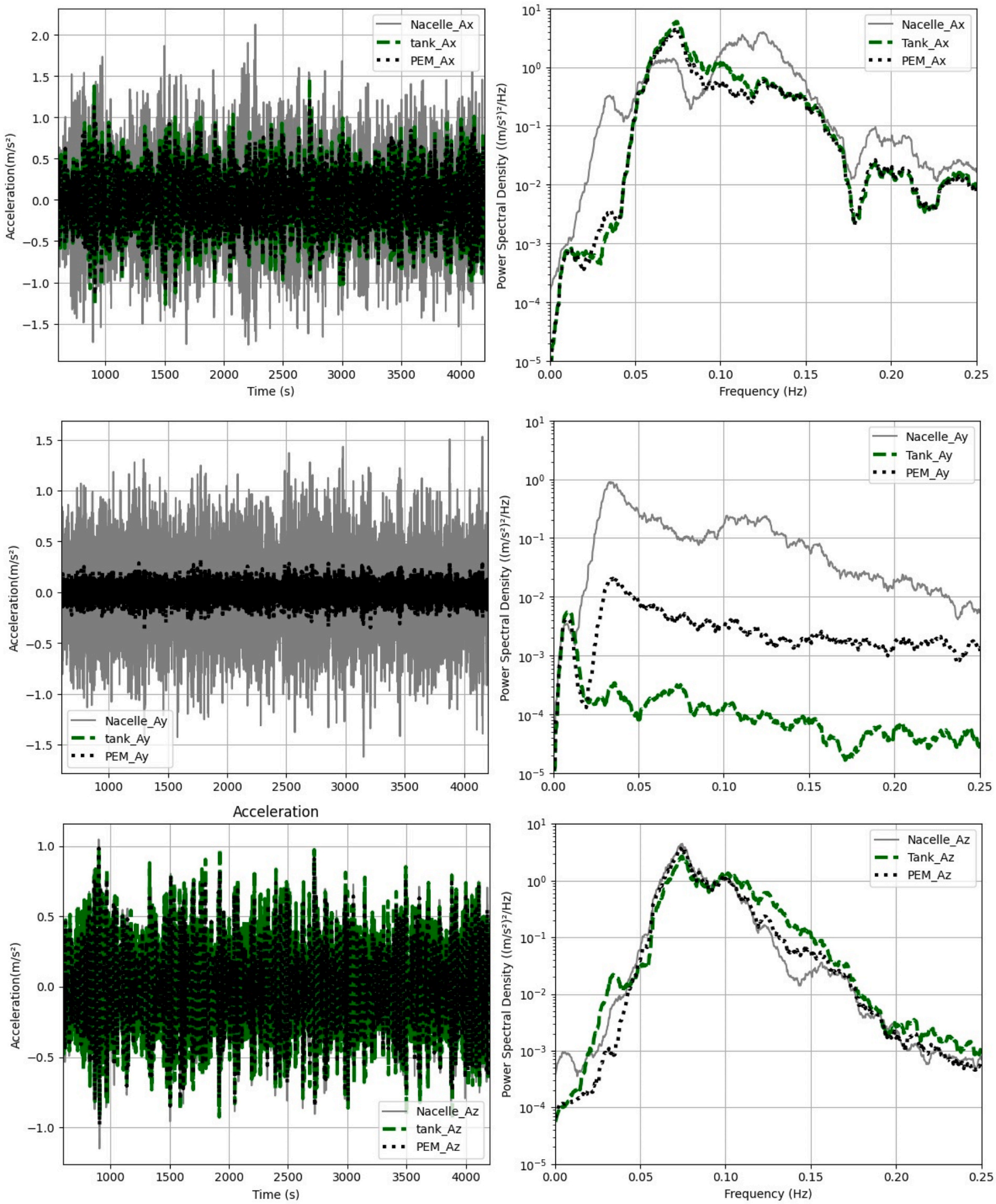

Fig. 8. Acceleration in the x, y, and z directions of the nacelle, hydrogen tanks, and PEM module at 47.5 m/s wind speed with irregular waves (Hs = 10.7 m, Tp = 14.2 s) and 8° nacelle yaw in DLC6.1 conditions; time domain on the left column and frequency domain on the right column.

mooring line tensions at the upwind mooring line increased slightly by approximately 3 %. This minor increase in loads, can be attributed to the pitch motion and altered dynamic response of the FWHS system. However, the observed differences are relatively small, indicating that the overall impact of the FWHS system on the mooring system performance is not significant. Nevertheless, it is crucial to consider these minor load increments during the design optimization process to ensure the long-term reliability and integrity of the mooring system.

Eliminating subsea power cables reduces both capital costs and installation time, offering clear advantages for offshore deployment. However, for large-scale wind farms, coordinating hydrogen offloading across multiple platforms poses logistical challenges. A dedicated fleet of transport vessels, equipped for rough sea conditions, is needed to operate within narrow weather windows. While detailed economic analysis is beyond this study, the concept presents a promising balance between simplified infrastructure and operational feasibility.

While this study assumes rigid, fixed hydrogen tanks for simplicity, practical deployments may involve structural flexibility under dynamic

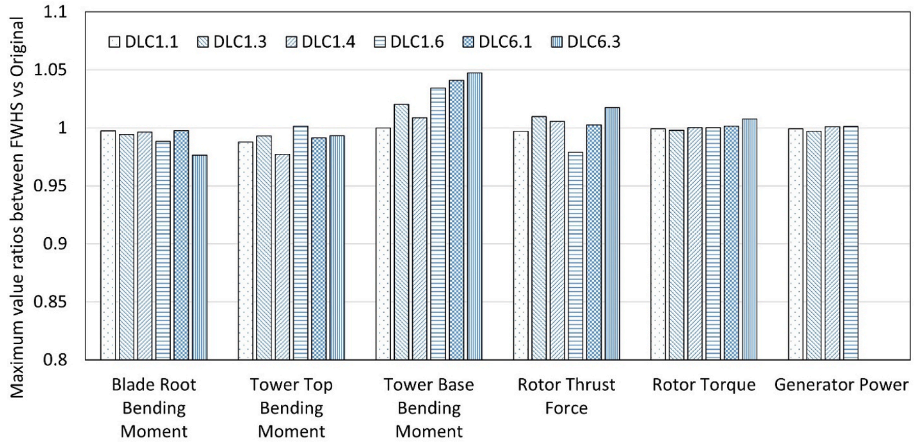

Fig. 9. Ratios of maximum loads and performance between FWHS model and original model.

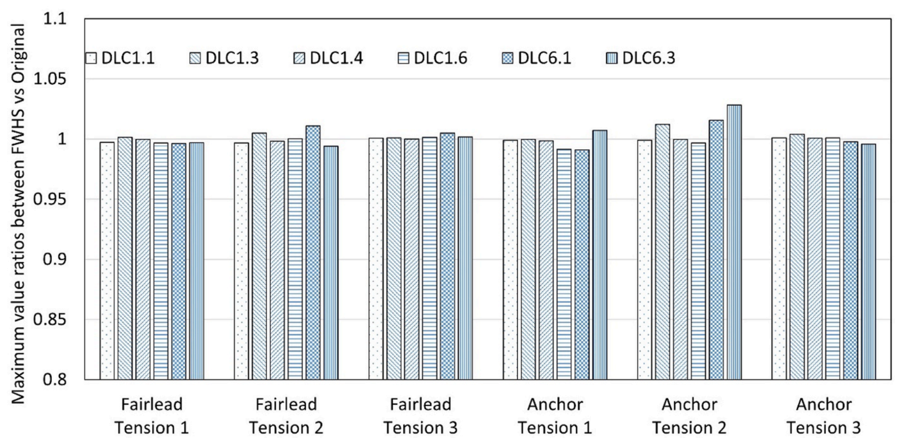

Fig. 10. Ratios of maximum fairlead tension and anchor tension of three mooring lines between FWHS model and original model.

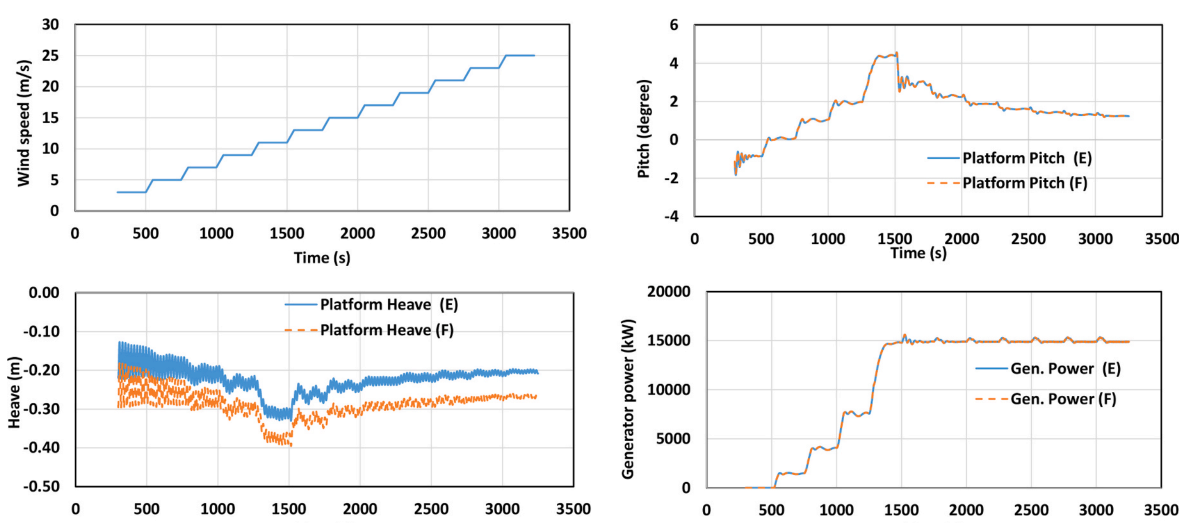

Fig. 11. Comparison between empty (E) and full (F) hydrogen storage tanks at different wind speeds, stepped from turbine cut-in to cut-out wind speed.

offshore conditions. Repetitive platform motions, thermal effects from compression, and periodic changes in tank mass during loading and unloading introduce cyclic stresses on the tank and its supports. These effects, not captured in the current model, may affect long-term fatigue performance. Future work should include detailed finite element modeling coupled with platform dynamics to assess structural reliability and design safety margins for fixable structures of hydrogen storage tanks.

6. Storage system effects

The tanks are loaded with 28,700 kg of hydrogen, representing 0.16 % of the total mass of the platform. To assess the impact of hydrogen loading and unloading, simulations of the floating system are conducted at different wind speeds, stepped up from cut-in to cut-out wind speed in order to monitor operational parameters. Fig. 11 displays a dynamic and performance comparison of the floating wind turbine system with the hydrogen storage either empty (E) or full (F). The analysis highlights differences in the platform pitch and heave motions, as well as variations in power generation over time across different wind speeds. A notable difference in the heave motion, approximately 0.063 m, is observed between the full and empty storage states due to the additional draft caused by the increased mass over the platform water plane area of 446.7 m^2. Despite these variations, the platform pitch and generated power follow similar trends in both storage conditions, rising with increasing wind speeds, indicating that hydrogen loading and unloading do not significantly alter the turbine system performance and operational efficiency.

7. Conclusion

This study presents a novel concept of integrating hydrogen production and storage systems into a 15 MW semi-submersible floating offshore wind turbine (FOWT). The proposed decentralized system offers a scalable and modular approach for maximizing offshore wind energy utilization. The following conclusions are drawn from the system design and dynamic performance evaluation:

- The integration of hydrogen production and storage systems resulted in a 4–5 % increase in pitch and roll inertia and a 6 % rise in the center of gravity of the platform, leading to moderate changes in platform dynamics. The maximum nacelle accelerations increased by less than 2 % in the x-direction and less than 10 % in the y-direction. The tower base bending moment experienced a slight increase, particularly under extreme wind and wave conditions, while blade root moment and tower top moment showed a slight reduction. The mooring line tensions at the upwind mooring line increased by approximately 3 %, though the surge and heave motions remained unchanged, indicating that the hydrogen system integration did not significantly alter the global platform response.
- The power output of the modified platform differed by less than 2 % from the original design across all load cases, demonstrating that the integration of hydrogen production and storage systems has minimal effect on wind energy harvesting. This result validates the effectiveness of the design in maintaining high operational efficiency while accommodating additional systems for hydrogen production and storage.
- Dynamic simulations with hydrogen storage tanks either full (28,700 kg at 70 MPa) or empty revealed negligible impacts on the operational parameters of the system. The difference in heave motion between these states was approximately 0.063 m, while pitch and power generation performance followed similar trends. The results demonstrate the platform's ability to maintain stable performance across different storage conditions and operational scenarios.
- The proposed decentralized hydrogen production and storage concept simplifies offshore wind farm deployment by removing the need for subsea cabling. This enables installation in remote areas without pipeline access and reduces infrastructure complexity. While the system demonstrates stable dynamic performance under various load conditions, future work should address operational logistics such as hydrogen offloading, risk assessment for high-pressure storage, and long-term economic feasibility.

The results confirm that integrating hydrogen production and high-pressure storage systems into a semi-submersible floating wind turbine can be achieved with minimal impact on platform dynamics and power performance. By eliminating the need for subsea cabling and maintaining stable operation under varying storage conditions, the proposed FWHS concept offers a technically feasible approach for decentralized offshore hydrogen production. Future research should focus on optimizing offloading logistics, enhancing safety for high-pressure storage, and conducting long-term dynamic analyses of flexible storage tank structures. In addition, economic evaluations considering various tank sizes, storage durations, and vessel unloading frequencies are essential to determine the optimal trade-off between system stability, logistical constraints, and overall project cost-effectiveness.

CRediT authorship contribution statement

Thanh Dam Pham: Visualization, Methodology, Writing – original draft, Validation, Conceptualization. **Van Nguyen Dinh:** Methodology, Conceptualization, Writing – original draft, Funding acquisition. **Luan Cong Trinh:** Methodology, Writing – original draft. **Frances Judge:** Formal analysis, Writing – original draft. **Paul Leahy:** Writing – original draft, Methodology, Conceptualization, Supervision, Funding acquisition.

Statement on the use of Generative Artificial Intelligence

Generative Artificial Intelligence was used to improve the written expression in this paper. All the text has been reviewed by the lead author and is approved by all authors.

Declaration of competing interest

The authors declare that they have no known competing financial interests or personal relationships that could have appeared to influence the work reported in this paper.

Acknowledgments

The research leading to this paper was supported through the HyFloat1 project, funded by Sustainable Energy Authority of Ireland (SEAI) under grant number RDD/709.

Appendix A. Supplementary data

Supplementary data to this article can be found online at https://doi.org/10.1016/j.ijhydene.2025.150832.

References

[1] Ram M, Bogdanov D, Aghahosseini A, Gulagi A, Oyewo AS, Odai Mensah TN, et al. Global energy transition to 100 % renewables by 2050: not fiction, but much needed impetus for developing economies to leapfrog into a sustainable future. Energy 2022;246:123419. https://doi.org/10.1016/j.energy.2022.123419.
[2] Hafner M, Tagliapietra S. Global Energy Transit: Rev Exist Literat 2020:1–24. https://doi.org/10.1007/978-3-030-39066-2_1.
[3] Rehman S, Alhems LM, Alam MdM, Wang L, Toor Z. A review of energy extraction from wind and ocean: technologies, merits, efficiencies, and cost. Ocean Eng 2023;267:113192. https://doi.org/10.1016/j.oceaneng.2022.113192.
[4] Lu X, McElroy MB, Kiviluoma J. Global potential for wind-generated electricity. Proc Natl Acad Sci 2009;106:10933–8. https://doi.org/10.1073/pnas.0904101106.
[5] Maxwell SM, Kershaw F, Locke CC, Conners MG, Dawson C, Aylesworth S, et al. Potential impacts of floating wind turbine technology for marine species and habitats. J Environ Manag 2022;307:114577. https://doi.org/10.1016/j.jenvman.2022.114577.
[6] Ambarita EE, Karlsen A, Osen O, Hasan A. Towards fully autonomous floating offshore wind farm operation & maintenance. Energy Rep 2023;9:103–8. https://doi.org/10.1016/j.egyr.2023.09.148.
[7] Farr H, Ruttenberg B, Walter RK, Wang Y-H, White C. Potential environmental effects of deepwater floating offshore wind energy facilities. Ocean Coast Manag 2021;207:105611. https://doi.org/10.1016/j.ocecoaman.2021.105611.
[8] Micallef D, Rezaeiha A. Floating offshore wind turbine aerodynamics: trends and future challenges. Renew Sustain Energy Rev 2021;152:111696. https://doi.org/10.1016/j.rser.2021.111696.

[9] Barooni M, Ashuri T, Sogut DV, Wood S, Taleghani SG. Floating offshore wind turbines: current status and future prospects. https://doi.org/10.3390/en16010002; 2022.

[10] Ehteshami SMM, Chan SH. The role of hydrogen and fuel cells to store renewable energy in the future energy network – potentials and challenges. Energy Policy 2014;73:103–9. https://doi.org/10.1016/j.enpol.2014.04.046.

[11] Singlitico A, Østergaard J, Chatzivasileiadis S. Onshore, offshore or in-turbine electrolysis? Techno-economic overview of alternative integration designs for green hydrogen production into Offshore Wind Power Hubs. Renew Sustain Energy Transit 2021;1(100005). https://doi.org/10.1016/j.rset.2021.100005.

[12] Rodríguez Castillo CA, Yeter B, Li S, Brennan F, Collu M. A critical review of challenges and opportunities for the design and operation of offshore structures supporting renewable hydrogen production, storage, and transport. Wind Energy Sci 2024;9:533–54. https://doi.org/10.5194/wes-9-533-2024.

[13] Zhang C, Shen L, Wu X, Shan F, Chen L, Liu S. Review of offshore superconducting wind power generation for hydrogen production. Energies (Basel) 2025;18(1889). https://doi.org/10.3390/en18081889.

[14] Ibrahim OS, Singlitico A, Proskovics R, McDonagh S, Desmond C, Murphy JD. Dedicated large-scale floating offshore wind to hydrogen: assessing design variables in proposed typologies. Renew Sustain Energy Rev 2022;160:112310. https://doi.org/10.1016/j.rser.2022.112310.

[15] Zhang M, Tao L, Nuernberg M, Rai A, Yuan Z-M. Conceptual design of an offshore hydrogen platform. Int J Hydrogen Energy 2024;59:1004–13. https://doi.org/10.1016/j.ijhydene.2024.02.077.

[16] Caine D, Wahyuni W, Pizii B, Iliffe M, Whitlock Z, Ryan B, et al. ERM Dolphyn hydorgen: phase 2–Final report. Environ Res Manage (ERM) 2021;106.

[17] Caine D, Iliffe M, Kinsella K, Wahyuni W, Bond L. Dolphyn hydrogen phase 1 final report. Manchester, United Kingdom: Environmental Resources Management; 2019.

[18] Dinh VN, Leahy P, McKeogh E, Murphy J, Cummins V. Development of a viability assessment model for hydrogen production from dedicated offshore wind farms. Int J Hydrogen Energy 2021;46:24620–31. https://doi.org/10.1016/j.ijhydene.2020.04.232.

[19] Choisnet T, Geschier B, Vetrano G. Initial comparison of concrete and steel hulls in the case of Ideol's square ring floating substructure. Proc 15th World Wind Energy Conf Exhibit 2016;31. Tokyo, Japan.

[20] Saitec R. SATH Technology—A competitive floating solution for offshore wind turbines suitable for shallow and deep waters. 2019 n.d.

[21] Roddier D, Cermelli C, Aubault A, Weinstein A. WindFloat: a floating foundation for offshore wind turbines. J Renew Sustain Energy 2010;2:33104. https://doi.org/10.1063/1.3435339.

[22] Pegalajar-Jurado A, Bredmose H, Borg M, Straume JG, Landbø T, Andersen HS, et al. State-of-the-art model for the LIFES50+ OO-Star Wind Floater Semi 10MW floating wind turbine. J Phys Conf Ser 2018;1104:012024. https://doi.org/10.1088/1742-6596/1104/1/012024.

[23] Allen CK, Allen CK, Viscelli A, Viscelli A, Dagher HJ, Dagher HJ, et al. Definition of the UMaine VolturnUS-S reference platform developed for the IEA wind 15-Megawatt offshore reference wind turbine. https://doi.org/10.2172/1660012; 2020.

[24] Huijs F, de Bruijn R, Savenije F. Concept design verification of a semi-submersible floating wind turbine using coupled simulations. Energy Proc 2014;53:2–12. https://doi.org/10.1016/j.egypro.2014.07.210.

[25] Skaare B. Development of the hywind concept. Int Conf Offshore Mech Arctic Eng 2017;57779. American Society of Mechanical Engineers.

[26] Utsunomiya T, Matsukuma H, Minoura S, Ko K, Hamamura H, Kobayashi O, et al. On. Sea Experiment of a Hybrid SPAR for Floating Offshore Wind Turbine Using 1/10 Scale Model. 2010. p. 529–36. https://doi.org/10.1115/OMAE2010-20730.

[27] Adam F, Myland T, Dahlhaus F, Großmann J. Scale tests of the GICON®-TLP for wind turbines. Int Conf Offshore Mech Arctic Eng 2014;45530. American Society of Mechanical Engineers.

[28] Oguz E, Clelland D, Day AH, Incecik A, López JA, Sánchez G, et al. Experimental and numerical analysis of a TLP floating offshore wind turbine. Ocean Eng 2018;147:591–605.

[29] Lucas TR, Ferreira AF, Santos Pereira RB, Alves M. Hydrogen production from the WindFloat Atlantic offshore wind farm: a techno-economic analysis. Appl Energy 2022;310. https://doi.org/10.1016/j.apenergy.2021.118481.

[30] Frensch SH, Fouda-Onana F, Serre G, Thoby D, Araya SS, Kær SK. Influence of the operation mode on PEM water electrolysis degradation. Int J Hydrogen Energy 2019;44:29889–98. https://doi.org/10.1016/j.ijhydene.2019.09.169.

[31] Devoy McAuliffe F, Judge FM, Murphy J. Modelling the installation of next generation floating offshore wind farms. Appl Energy 2024;374:124001. https://doi.org/10.1016/j.apenergy.2024.124001.

[32] Guanche R, Martini M, Jurado A, Losada IJ. Walk-to-work accessibility assessment for floating offshore wind turbines. Ocean Eng 2016;116:216–25. https://doi.org/10.1016/J.OCEANENG.2016.03.013.

[33] O'Connor M, Lewis T, Dalton G. Weather window analysis of Irish and Portuguese wave data with relevance to operations and maintenance of marine renewables. Proceedings of the ASME 2013 32nd international conference on ocean. Offshore and Arctic Engineering; 2013.

[34] Cullinane M, O'Connell R, Murphy J. Data-driven assessment of the Survivability and Maintainability of Offshore renewable energy devices in Ireland's harsh maritime climate. OCEANS 2023 - limerick. 2023. p. 1–7. https://doi.org/10.1109/OCEANSLimerick52467.2023.10244392. Limerick.

[35] Gaertner E, Rinker J, Sethuraman L, Zahle F, Anderson B, Barter GE, et al. IEA wind TCP task 37: definition of the IEA 15-Megawatt offshore reference wind turbine. United States, https://doi.org/10.2172/1603478; 2020.

[36] Siemens Energy. Silyzer 300: the next paradigm of PEM electrolysis n.d. https://p3.aprimocdn.net/siemensenergy/3baa4ffa-f1f1-422f-a770-b08300c0f2b0/Datasheet-Silyzer300-pdf_Original%20file.pdf. [Accessed 21 August 2024].

[37] Wang T, Cao X, Jiao L. PEM water electrolysis for hydrogen production: fundamentals, advances, and prospects. Carbon Neutrality 2022;1:21. https://doi.org/10.1007/s43979-022-00022-8.

[38] Sdanghi G, Maranzana G, Celzard A, Fierro V. Review of the current technologies and performances of hydrogen compression for stationary and automotive applications. Renew Sustain Energy Rev 2019;102:150–70. https://doi.org/10.1016/j.rser.2018.11.028.

[39] Maximator. MAX Compression System 2.0 2024. https://www.maximator-hydrogen.de/en/product-portfolio/max-compression-system-20-75-kw. [Accessed 21 October 2024].

[40] Cheng Q, Zhang R, Shi Z, Lin J. Review of common hydrogen storage tanks and current manufacturing methods for aluminium alloy tank liners. Int J Lightweight Mater Manuf 2024;7:269–84. https://doi.org/10.1016/j.ijlmm.2023.08.002.

[41] Moriarty PJ, Hansen AC. AeroDyn theory manual. Renew Energy 2005., NREL/TP-500-36881.

[42] Hall M, Goupee A. Validation of a lumped-mass mooring line model with DeepCwind semisubmersible model test data. Ocean Eng 2015;104:590–603. https://doi.org/10.1016/J.OCEANENG.2015.05.035.

[43] Jonkman JM, Buhl Jr ML. Fast User's guide updated August 2005. https://doi.org/10.2172/15020796; 2005.

[44] Jonkman BJ. TurbSim user's guide v2. 00.00. National Renewable Energy Laboratory-NREL; 2014.

[45] Pham TD, Trinh LC, Dinh VN, Leahy P. Conceptual design of a hybrid floating offshore wind turbine integrated with hydrogen production and storage system. Ocean renewable energy, ume 7. American Society of Mechanical Engineers; 2024. https://doi.org/10.1115/OMAE2024-121580.